ADVANCED MATERIALS

Supporting Information

for *Adv. Mater.*, DOI: 10.1002/adma.201600466

Tough Physical Double-Network Hydrogels Based on Amphiphilic Triblock Copolymers

*Hui Jie Zhang, Tao Lin Sun, Ao Kai Zhang, Yumihiko Ikura, Tasuku Nakajima, Takayuki Nonoyama, Takayuki Kurokawa, Osamu Ito, Hiroyuki Ishitobi, and Jian Ping Gong**

Supporting Information

Tough physical double network hydrogels based on amphiphilic tri-block copolymers

*Hui Jie Zhang, Tao Lin Sun, Ao Kai Zhang, Yumihiko Ikura, Tasuku Nakajima, Takayuki Nonoyama, Takayuki Kurokawa, Osamu Ito, Hiroyuki Ishitobi, and Jian Ping Gong**

Measurements

Water content measurement

The water content of the gel was measured using a moisture balance MOC-120H (Shimadzu Co.). The dry sample was obtained by heating the sample to 120 °C

Tensile test

Uniaxial tensile tests were performed on dumbbell-shaped gels with the standard JIS-K6215-7 size (35 mm (L) × 2 mm (w) × 1 mm (d)) using a Tensilon RTC-1310 (Orientec Co.) tensile tester. The initial distance L_0 between the two clamps of the tester was 12 mm and the tensile deformation was performed at the rate of 0.14 s^{-1} unless specifically indicated. Cyclic tensile tests were also performed on the same samples at the rate of 0.14 s^{-1} with maximum strain of 1 mm/mm.

Pure shear test

Pure shear test was applied to characterize the toughness, following the method described in references [9, 30, 31]. For one sample, two different shapes of the sample, notched and unnotched, were used to measure the tearing energy T. The samples were cut into a rectangular shape with a width of 20 mm and length 40 mm (a_0) with thickness of 0.71 mm (b_0 = 0.71 mm). An initial notch of 10 mm in length was cut using a razor blade. The test

sample was clamped on two sides, and the initial distance between the two clamps was fixed at 8 mm (L_0). The lower clamp was pulled upward at constant velocity of 100 mm/min, while the upper clamp was fixed. The force-length curves of the samples were recorded, and the tearing energy was calculated from $T = U(L_c)/(a_0 \times b_0)$, where L_c is the distance between the two clamps when the crack starts to propagate in the notched sample, and $U(L_c)$ is the work done by the applied force to the unnotched sample at the critical stretching distance L_c. The onset of the crack propagation was determined using the movie image recorded by a camera.

Rheological test

Rheological tests were performed using an ARES rheometer (advanced rheometric expansion system, Rheometric Scientific Inc.). The disc-shaped samples with thicknesses of ~1 mm and diameters of 15 mm were adhered to the plates with glue and surrounded by water.

The rheological temperature-frequency sweep test was performed with frequency sweep from 0.628 to 100 rad/s and a shear strain of 0.1% in the parallel-plates geometry with fixed gap distance during test in a temperature range of 1–81 °C. As the top and bottom of tested gel was fixed on the parallel-plates by glue, the volume of gel during measurement is considered as being fixed. Thus following the time-Temperature Superposition principle for the construction of the master curve, the modulus-scale shift factor b_T was set as 1.

The rheological temperature sweep test was performed at frequency of 6.28 rad/s, temperature range of 0.1-95 ^{o}C and heating rate of 1 ^{o}C/min. The apparent activation energy E_a is obtained from an Arrhenius equation: $a_T = Ae^{E_a/RT}$, where a_T is the shift factor, R is the ideal gas constant, and A is a constant.[9]

Fourier transform infrared spectroscopy (FT-IR)

FT-IR was measured by MFT-2000 micro sampling FTIR spectrometer (JASCD Corp.). The testing scale was from 400-4000 cm^{-1}, with the resolution of 4 cm^{-1}.

SAXS analysis

SAXS measurements were performed at the SPring-8. The wave length of X-ray was 1.0 Å and the cameral length was 2 m. The data acquisition time was 20 s for the SAXS pattern and the two dimensional (2D) scattering images were analyzed with Fit2D software from European Synchrotron Radiation Facility.

Mechanical property of B-DN gel with different concentration of AAm in the precursor solution of the second network

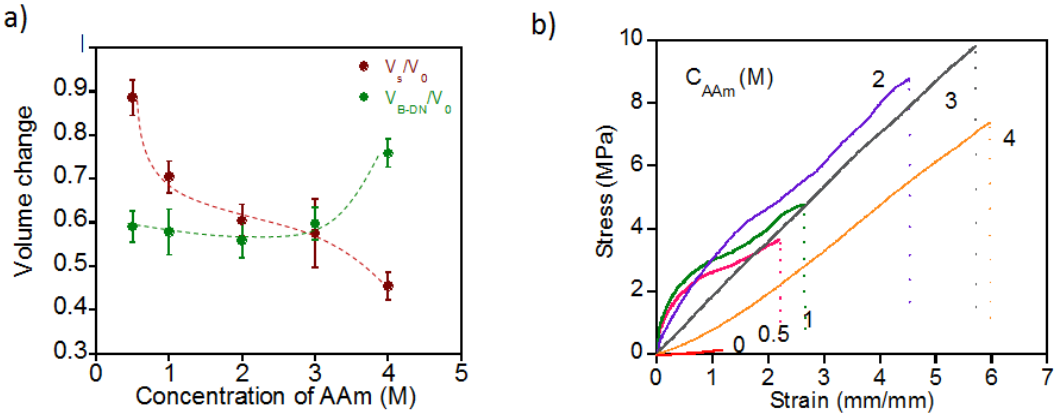

Figure S1. a) Volume change of block copolymer gel (B-gel) after being immersed in AAm solution and forming equilibrium B-DN gel; V_0 and V_s are the volume of B-gel in water and in AAm solution, respectively. $V_{B\text{-}DN}$ is the volume of equilibrium B-DN gel in water. b) Tensile test results of equilibrium B-DN gels with different AAm concentration of precursor solution.

Table S1. Water content and mechanical property of B-DN gels with different AAm concentration of precursor solution.

Gels	C_{AAm} (M)	C_{wt} (%)	E (MPa)	σ_b (MPa)	ε_b (mm/mm)	Fracture energy (kJ/m^2)
B gel	0	82±1	0.051±0.04	0.19±0.04	0.97±0.2	0.063±0.07
B-DN0.5	0.5	54±2	5.8±0.1	3.4±0.2	2.3±0.3	0.91±0.09
B-DN1	1	46±2	14.2±0.9	5.5±0.5	3.2±0.4	1.82±0.19
B-DN2	2	45±2	7.1±0.5	7.5±1.1	3.6±0.7	2.22±0.22
B-DN3	3	44±2	2.2±0.2	10.5±1.4	5.7±0.7	2.85±0.22
B-DN4	4	57±4	0.59±0.08	6.4±2.5	5.8±1.6	1.32±0.07

C_{wt}, E, σ_b, and ε_b stand for water content, elastic modulus, fracture stress, and fracture strain, respectively. All the data are averages for 3 experimental tests.

Structure characterization of B gel

The 2 D SAXS scattering pattern of B gel shows isotropic circles, as shown in Figure S2a, which indicates isotropic structure of B gel. The 1-D SAXS profile shows several peaks at high scattering vector q.

Thus in this study, the SAXS 1D profile is fitted by the Percus-Yevick disordered hard-sphere model, in which the gel is modeled as a liquid with interacting hard spheres[24-26]. In this model, the scattering intensity is given by

$$I(q) = KNP(q)S(q)$$

where K is a constant, N is the number of scattering centers, $S(q)$ stands for structure factor which accounts for the interaction of particles and corresponds to the low q peak, and $P(q)$ stands for form factor corresponding to high q peaks. The SAXS profile was fitted according to the work of Kinning and Thomas[24], with parameters of R_{HS} and η, where R_{HS} refers to the radius of the fictitious hard sphere which contains the spherical hydrophobic domain and some surrounded molecules and η refers to the volume fraction of hard sphere .

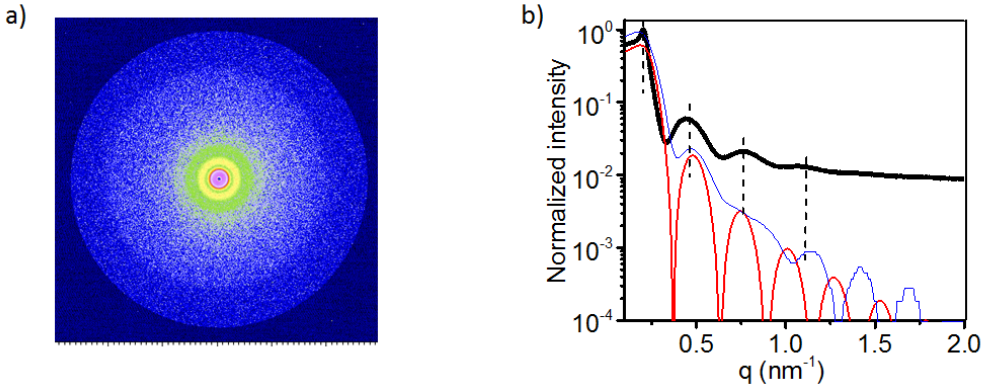

Figure S2. a) Small angel X-ray scattering patterns of B gel. b) SAXS profile of B gel with normalized intensity vs q. The black line is the tested data; the red line is Percus-Yevick fit with parameters R_{HS} = 12.2nm, η = 0.21; and the blue line is Percus-Yevick fit considering the size distribution of hard sphere with parameters of R_{HS} = 12.2nm, η = 0.21, σ = 1.4, where σ is variance of R_{HS} in Gaussian distribution.

From the q value of the first peak which correspond to the structure factor, the average inter domain distance d was calculated as $d = 2\pi/q_{max}$ = 31.2 nm. The number density of hydrophobic domain was estimated as $\nu_h \approx \frac{1}{\frac{4}{3}\pi\left(\frac{d}{2}\right)^3}$. As the micelles act like cross-linking points and the mechanical response is dominated by the stretching of the mid-block chains at small strain, the modulus E of B gel can be described using rubber elasticity. Thus the chain number density of B gel υ is able to be estimated from $E = 3\upsilon k_B T$, where $k_B T$ is the thermal energy.[33] In this way, the average number f of polymer chains in one hydrophobic domain was able to be estimated as $f = \upsilon/2\nu_h \approx 33$.

Estimation of the stability of hydrogen bonds pairs in B-DN gel

To estimate the sable structure of hydrogen bonding pair, final heat of hydrogen bonding formation was calculated by semi-empirical molecular orbital method using MOPAC2007. Firstly, the AAm and MAA monomers were modeled on Winmostar software, and the individual stable structures were calculated. Then, the possible pairs of the optimized monomers for forming hydrogen bonds were made. The initial distances of hydrogen bonds (N-H···O, O-H···O), were 0.289 nm (N to O length), 0.272 nm (O to O), respectively. For all simulations of single monomers and monomer pairs, we applied keywords of PM7, EF, PRECISE, GNORM = 0.05, NOINTER, GEO-OK, MMOK, EPS = 80.4 and NSPA = 162.

Table S2. The calculated final heat of the formation of possible hydrogen bonding pairs in the system containing MAA, AAm in water condition.

Number of Bond	Form	HOF [kcal/mol]
4	2[MAA···2(H_2O)], 2AAm	-544.3378
4	2[AAm···2(H_2O)], 2MAA	-534.64924
4	2(MAA···H_2O), 2(AAm···H_2O)	-545.1455
4	**2(MAA···AAm), 2(H_2O···H_2O)**	**-551.76316**
4	MAA···MAA, AAm···AAm, 2(H_2O···H_2O)	-550.18121
5	2[MAA···2(H_2O)], AAm···AAm	-551.09772

5	2[AAm···2(H_2O)], MAA···MAA	-546.98145
5	MAA···2(H_2O), AAm···2(H_2O), MAA···AAm	-549.83056

As shown in Table S2, in the system contains MAA and AAm in water, the lowest final heat of formation was obtained when the hydrogen bonds between AAm and MAA formed, indicating that the hydrogen bonding between the amide group of PAAm and carboxylic acid group of PMAA is the most stable in aqueous conditions.

Mechanical property comparison of B-DN and chemically crosslinked PMAA/PAAm DN gel (c-DN gel)

Synthesis of c-DN gels: Firstly, the chemically crosslinked PMAA gels (c gels) were synthesized by radical polymerization under UV for 8h with the composition that MAA 3 M, 2-oxoglutaric acid 0.02 mol %, and varied MBAA of 0.005 M, 0.011 M, 0.03 M, 0.04 M, 0.05 M, 0.066 M, which correspond to the average partial chain lengths of 600, 273, 100, 75, 60, 45 in degree of polymerization *N*, respectively. Then, the c gel was immersed in AAm solution (AAm 3 M, 2-oxoglutaric acid 0.02 mol %) for 3 days. The polymerization of the second network was carried out by exposing the gels under UV for 8 h to get the as-prepared gels. The as-prepared gels were equilibrated in water for more than 4 days. The c gels and their c-DN gels were coded as c-*N* gels and c-*N*-DN gels where *N* stands for the average partial chain lengths of the first network.

The c-DN gels also possess the sacrificial hydrogen bonds between PAAm and PMAA first network and no chemical cross-linker was added during the polymerization of the second network.

In Figure S3d, the B gel shows the same elastic modulus with the c-273 gel that has the same

average partial chain length N of PMAA as that of B gel. This result can be understood as follows. In B gel, the weight percent of PMAA is $C_{PMAA\,(B)} = 6.9\%$; and in c-273 gel the weight percent of PMAA is $C_{PMAA\,(c-273)} = 13.9\%$. So, the number densities of the PMAA chains in B gel and c-273 gel has a relation of $\upsilon_{B\,gel} \cong \frac{1}{2}\upsilon_{c-273\,gel}$. According to the Phantom model, $E = 3\upsilon k_B T\frac{f-2}{f}$, where υ is number density of chains.[33] For B gel $f \cong 33$ and for c gel $f = 4$. So $E_{B\,gel} \cong 3\upsilon_{B\,gel}k_B T$ and $E_{c-273} = 3\upsilon_{c-273}k_B T \times \frac{1}{2}$. As $\upsilon_{B\,gel} \cong \frac{1}{2}\upsilon_{c-273\,gel}$, one gets $E_{B\,gel} = E_{c-273\,gel}$, in agreement with the observation. This result indicates that the B gel follows rubber elasticity theory and the hydrophobic domains act as cross-linkers with high functionality.

Even using the first network of the same elastic modulus and AAm concentration in the precursor solution, the B-DN gel shows much higher elastic modulus comparing to the c-DN gel (as shown in Figure S3d). This result indicates that more large amount of additional physical crosslinking was formed in the B-DN gels than in c-DN gels. Accordingly, the hydrophobic domains of the first network in B-DN gels substantially enhance the formation of the hydrogen bonds, and the density of hydrogen bonds in B-DN gel is much higher than in the c-DN gels.

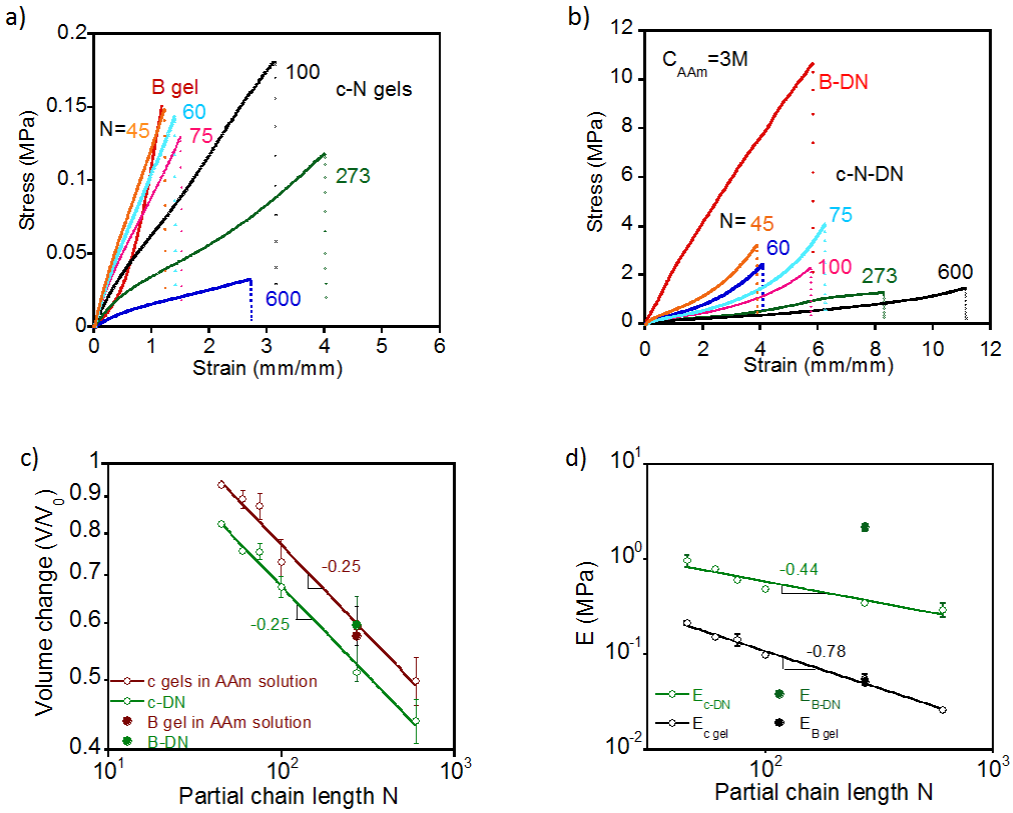

Figure S3. a) Tensile test of B gel and chemically cross-linked PMAA gels (c-*N* gels). b) Tensile test of B-DN gel and c-*N* DN gels. The latter is the DN gel using the chemically crosslinked PMAA as the first network. The '*N*' in a) and b) stands for the average partial chain length *N* of the c gel network. c) Volume change as function of partial chain length of PMAA of c gels and B gel after being immersed in AAm solution and forming c-DN gels and B-DN gel, where V_0 refers to the volume of the first network gels in water. d) Elastic modulus of c gels, B gel, c-DN gels and B-DN gel as function of the partial chain length *N*.

Heating-cooling induced recovery of B-DN gel

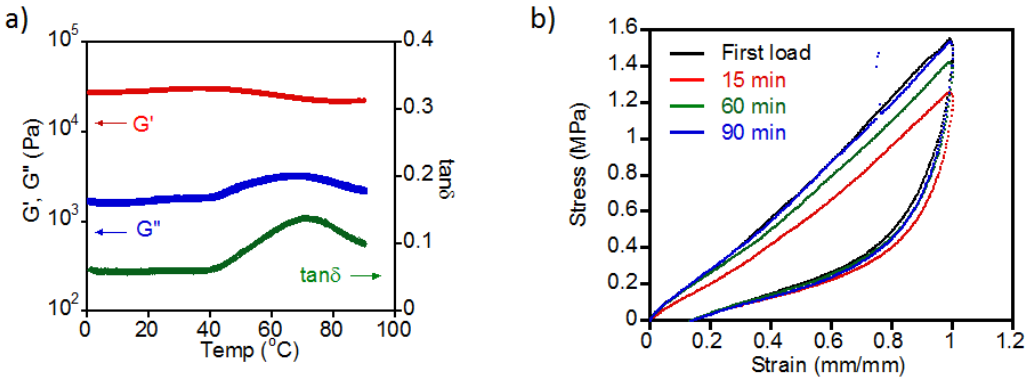

Figure S4. a) Temperature dependence of the storage modulus (*G'*), loss modulus (*G"*) and loss factor (*tanδ*) of B gel at 6.28 rad/s and 0.1% strain. b) Waiting time dependence of recovery of B-DN3 gel at room temperature after being heated at 60 ^{o}C for 1min.

Stability of B-DN gel in concentrated saline solution

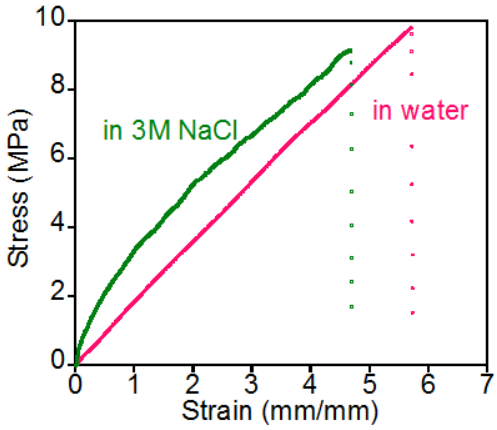

Figure S5. Tensile stress-strain curves of B-DN3 gel equilibrated in water and in 3M NaCl solution for 3 days, respectively.

Fracture energy and Young's modulus of various materials

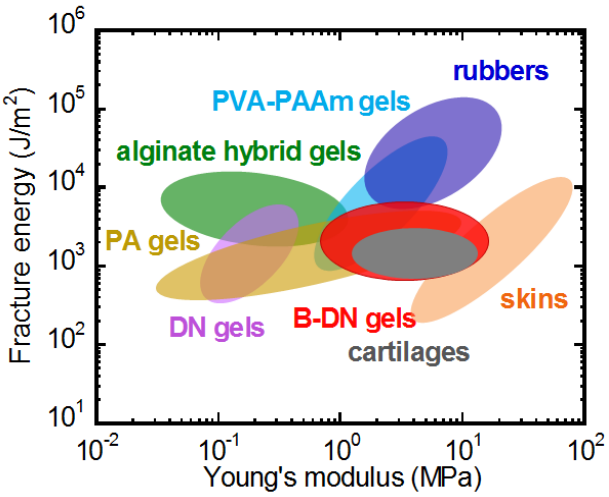

Figure S6. Fracture energy and Young's modulus of various materials. [19-22, 27-29]